Pictorial Essay | Musculoskeletal Imaging

http://dx.doi.org/10.3348/kjr.2014.15.4.508
pISSN 1229-6929 · eISSN 2005-8330
Korean J Radiol 2014;15(4):508-522

Korean Journal of Radiology
KJR

Anatomy, Variants, and Pathologies of the Superior Glenohumeral Ligament: Magnetic Resonance Imaging with Three-Dimensional Volumetric Interpolated Breath-Hold Examination Sequence and Conventional Magnetic Resonance Arthrography

Hayri Ogul, MD[1], Leyla Karaca, MD[1], Cahit Emre Can, MD[2], Berhan Pirimoglu, MD[1], Kutsi Tuncer, MD[2], Murat Topal, MD[2], Aylin Okur, MD[1], Mecit Kantarci, MD, PhD[1]

Departments of [1]Radiology and [2]Orthopedic, Medical Faculty, Ataturk University, Erzurum 25090, Turkey

The purpose of this review was to demonstrate magnetic resonance (MR) arthrography findings of anatomy, variants, and pathologic conditions of the superior glenohumeral ligament (SGHL). This review also demonstrates the applicability of a new MR arthrography sequence in the anterosuperior portion of the glenohumeral joint. The SGHL is a very important anatomical structure in the rotator interval that is responsible for stabilizing the long head of the biceps tendon. Therefore, a torn SGHL can result in pain and instability. Observation of the SGHL is difficult when using conventional MR imaging, because the ligament may be poorly visualized. Shoulder MR arthrography is the most accurately established imaging technique for identifying pathologies of the SGHL and associated structures. The use of three dimensional (3D) volumetric interpolated breath-hold examination (VIBE) sequences produces thinner image slices and enables a higher in-plane resolution than conventional MR arthrography sequences. Therefore, shoulder MR arthrography using 3D VIBE sequences may contribute to evaluating of the smaller intraarticular structures such as the SGHL.

Index terms: *Superior glenohumeral ligament; Anterosuperior impingement; Shoulder; MR arthrography; VIBE sequence*

INTRODUCTION

The glenohumeral joint is a major joint of the human body. It is the most commonly dislocated joint because of the large size of the humeral head compared to the small size of the glenoid fossa (1). The glenohumeral ligaments (GHLs), joint capsule, and glenoid labrum are parts of the passive stabilizing mechanisms of the glenohumeral joint. The GHLs are localized thickenings of the glenohumeral joint capsule that extend from the anterior and inferior glenoid margin of the joint to the anatomical neck of the humerus. Three ligaments have been described: the superior glenohumeral ligament (SGHL), the middle glenohumeral ligament (MGHL), and the inferior glenohumeral ligament (IGHL) complex, which are composed of an anterior band, a posterior band, and an axillary recess. The main two functions of the GHLs are to avoid superior-inferior translation and to maintain anterior stability (2). Magnetic resonance (MR) imaging of the shoulder without intraarticular contrast medium can be used to observe some anatomical structures, such as the bony components, biceps tendon, and rotator cuff tendons. However, MR arthrography is mostly used for demonstrating abnormal GHLs, and it is the most accurate imaging technique established (3).

Received December 13, 2013; accepted after revision April 13, 2014.

Corresponding author: Mecit Kantarci, MD, PhD, Department of Radiology, Medical Faculty, Ataturk University, 200 Evler Mah. 14. Sok No 5, Dadaskent, Erzurum 25090, Turkey.
• Tel: (90) 442 2316666-6751 • Fax: (90) 442 3166333
• E-mail: drhogul@gmail.com

Korean Journal of Radiology
KJR

The SGHL is the most important structure in the anterosuperior part of the glenohumeral joint capsule (4, 5). It plays essential roles in anterosuperior impingement syndrome and in stabilizing the long head of the biceps tendon (LHBT). Thus, radiologists should observe the SGHL and coexistent pathologies in patients presenting with pain at the anterosuperior section of the shoulder. The purpose of this study was to review the normal MR arthrography anatomy and variants of this important ligament. We also discussed about its basic biomechanics and illustrated examples of injuries involving this ligament.

Arthrography Procedure

Different methods of injections into the glenohumeral joint for diagnostic arthrography have been previously described. These methods involve fluoroscopy, ultrasonography, and computed tomography, as well as techniques other than image-guiding. For sonographic guidance, the use of ionizing radiation and iodinated contrast materials are avoided.

There are various approaches for glenohumeral joint MR arthrography. Although the anterior approach is the most commonly used, the posterior and the rotator interval approaches have recently been preferred (6-8). Both the posterior and rotator interval approaches are used at our institution via ultrasonography guidance. In the posterior approach, a transducer is placed over the long axis of the myotendinous junction of the infraspinatus muscle, and it is angled to show the contours of the posterior glenoid rim, posterior glenoid labrum, and posteromedial portion of the humeral head. The needle is introduced in a lateral to medial direction, obliquely from the skin to the glenohumeral joint space and parallel to the long axis of the transducer (Fig. 1) (7). In the rotator interval approach, the coracoid process and the adjacent superomedial subchondral aspect of the humeral head are observed with a high frequency linear probe in a plane transverse to the joint line. The needle entry point is just superior to the subscapularis tendon and lateral to the coracoid process. The needle is advanced freehand, from medial to lateral, obliquely from the skin surface to the humeral head within the imaging plane of the transducer, until the tip reaches the cartilage of the humeral head (Fig. 2).

Imaging Techniques

A direct MR arthrography of the glenohumeral joint after intraarticular injection of diluted gadolinium chelates is the preferred imaging technique for the evaluation of the labroligamentous complex and joint capsule (9, 10). Observation of the GHLs is difficult when using conventional

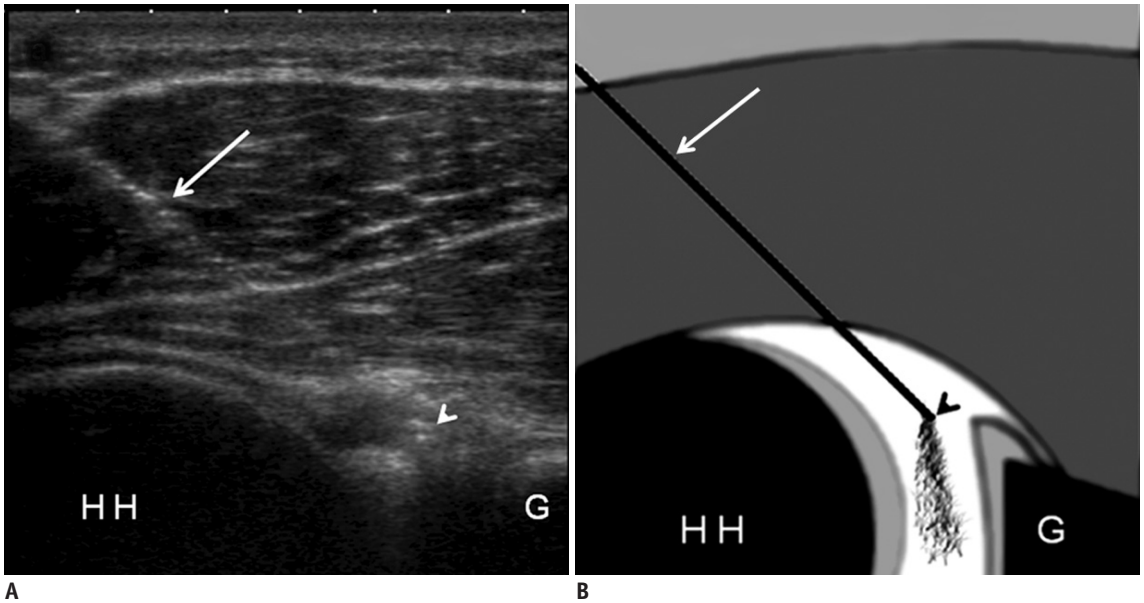

A B

Fig. 1. Ultrasonography-guided posterior injection technique for shoulder MR arthrography.
A. Transverse ultrasonography image shows needle track and intraarticular needle tip in patient with posterior glenohumeral joint puncture for MR arthrography. It also reveals distention of joint capsule with free fluid within joint space. White arrow = needle shaft, white arrowhead = intraarticular needle tip. **B.** Corresponding schematic drawing shows optimal needle track and placement. White arrow = needle shaft, black arrowhead = intraarticular needle tip. G = posterior glenoid rim, HH = humeral head

shoulder MR imaging, because these ligaments may be poorly visualized or may mimic labral lesions (9, 11). Chung et al. (12) presented a cadaveric study comparing conventional MR imaging to MR arthrography of the same shoulder joint. In this study, the SGHL was not identified by conventional MR imaging, in all of the cases; however, it was identified by direct MR arthrography, in all of the cases. At our institution, we prefer direct MR arthrography for the identification of the labroligamentous complex.

At our institution, MR arthrography and conventional MR imaging examinations are performed with a 1.5-T or 3-T MR scanner (Magnetom Avanto or Magnetom Skyra; Siemens Healthcare, Berlin, Germany) within 15 minutes after the injection. Our MR arthrography protocol uses fat-suppressed

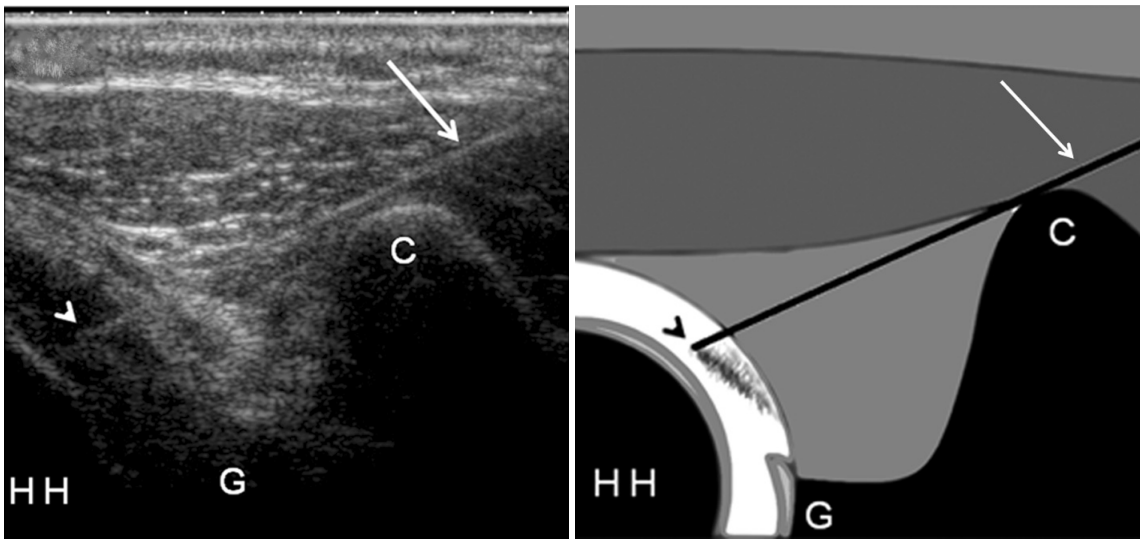

A B

Fig. 2. Ultrasonography-guided rotator interval injection technique for shoulder MR arthrography.
A. Axial oblique ultrasonography image, obtained at anterosuperior aspect of glenohumeral joint, shows needle track (white arrow) and intraarticular needle tip (white arrowhead) in patient with rotator interval puncture for MR arthrography. Image also shows distention of joint capsule with free fluid within joint space. **B.** Corresponding schematic drawing shows optimal needle track and placement. White arrow = needle shaft, black arrowhead = intraarticular needle tip. C = coracoid process, G = anterior glenoid rim, HH = humeral head

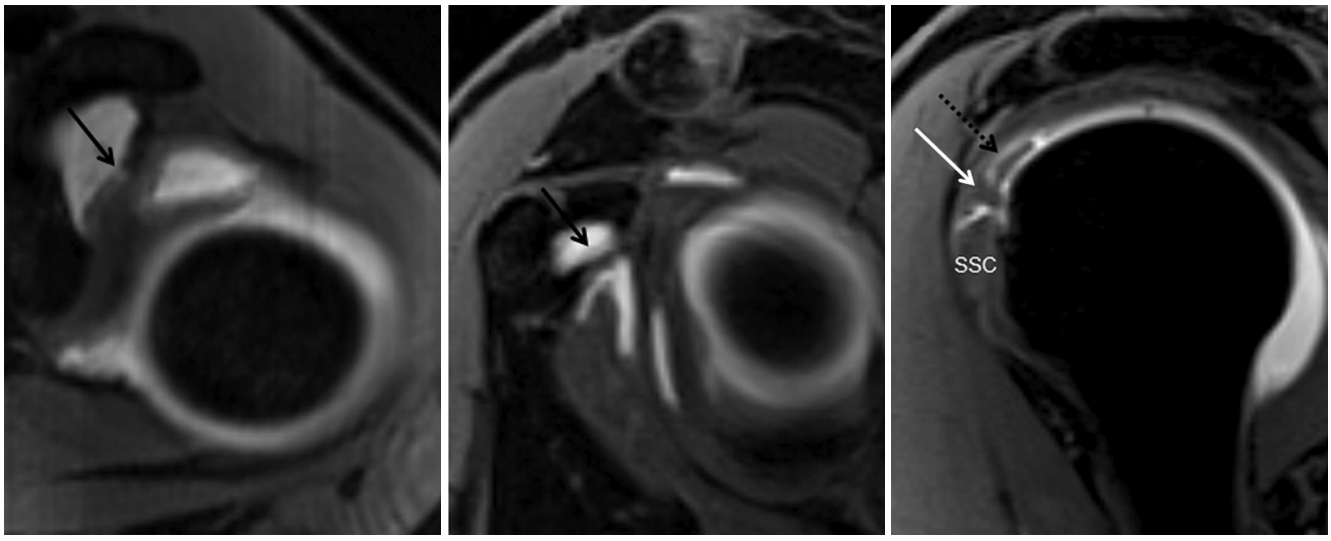

A B C

Fig. 3. Normal arthrographic anatomy of SGHL in 51-year-old male who suffered from shoulder pain.
A. Axial reformatted image of fat-suppressed 3D VIBE sequence shows SGHL (black arrow). **B.** Oblique sagittal reformatted image of fat-suppressed 3D VIBE sequence shows SGHL (black arrow) underneath coracoid process. **C.** Oblique sagittal fat-saturated 3D VIBE MR arthrographic image shows normal anatomic appearance of pulley sling. SGHL (white arrow) wraps around horizontal portion of LHBT (black dotted arrow), which is at distance from subscapularis tendon (SSC). LHBT shows normal diameter and signal intensity. LHBT = long head of biceps tendon, SGHL = superior glenohumeral ligament, 3D VIBE = three-dimensional volumetric interpolated breath-hold examination

Korean Journal of Radiology
KJR

spin-echo (SE) T1-weighted images. This is performed in the axial, oblique coronal, and oblique sagittal planes, with surface coils placed around the shoulder joint (650/15, echo train length 8 mm, section thickness 3 mm, spacing 0.3 mm, field of view [FOV] 16 cm^2, matrix 256 x 250, 3 signals acquired). In our clinical practice, a fat-suppressed three dimensional (3D) volumetric interpolated breath-hold examination (VIBE) sequence (repetition time/echo time 13.2/4.7 msec, flip angle 11°, 160 x 160 mm FOV, matrix 512 x 512, one slab of 112 slices with a slice thickness of 0.6 mm, and one acquisition) is also added to the shoulder MR arthrography scanning protocol, after the T1-weighted SE fat-suppressed sequences are acquired. Fat-suppressed 3D VIBE sequence imaging is a relatively new spoiled gradient-echo protocol that provides fast low angle images.

The use of 3D VIBE sequences produces thinner image slices with the thickness of 0.6 mm, which enhances effectiveness of the imaging. Volume acquisition enables multiplanar image reconstruction and volume rendering. It also provides good contrast between the glenoid and surrounding soft tissues in MR arthrography of the glenohumeral joint.

Normal Anatomy of the Superior Glenohumeral Ligament

Anatomical knowledge of the labroligamentous structures is crucial to the diagnosis of abnormalities revealed by MR

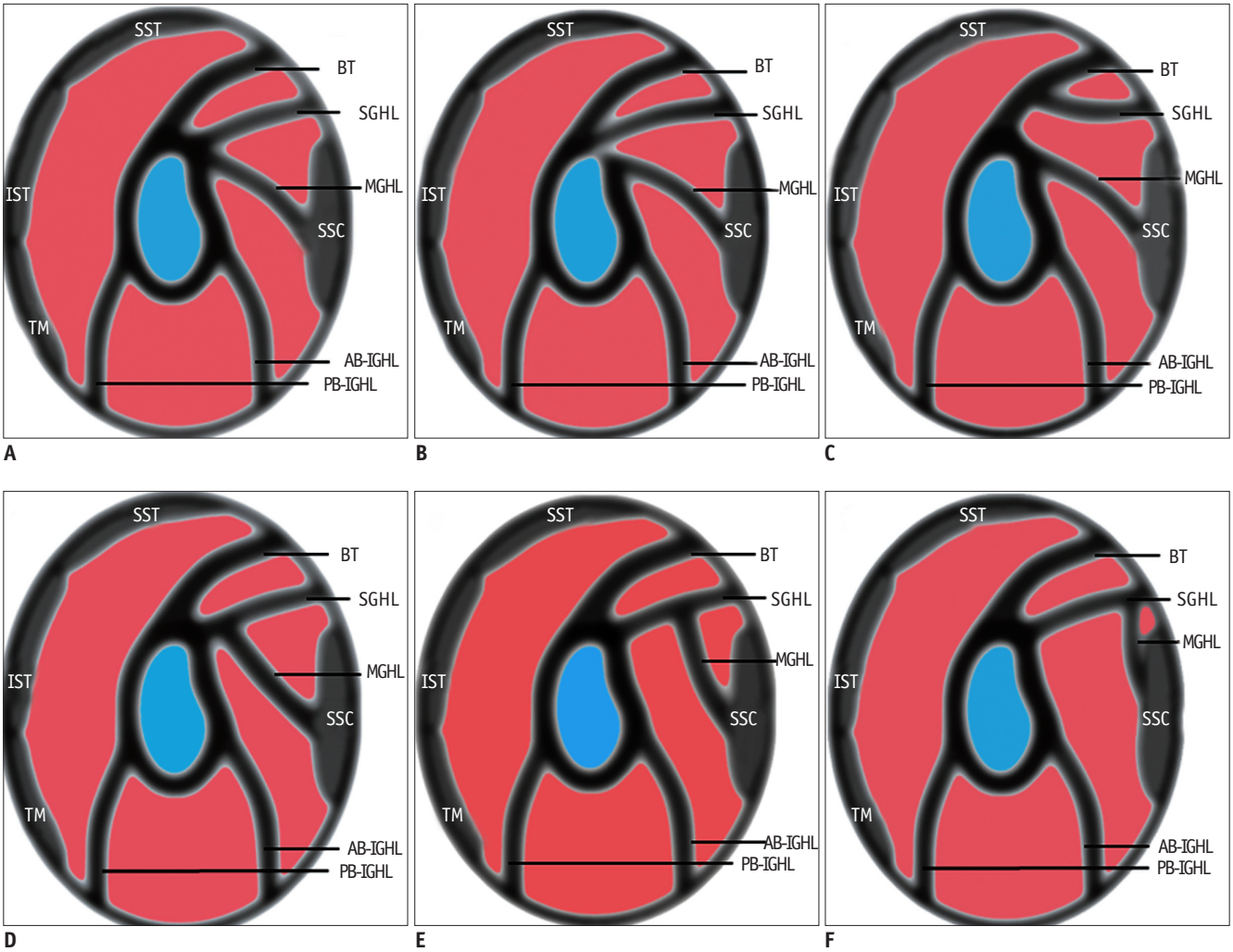

Fig. 4. Types of SGHL origination.
A. Drawing (lateral view) shows normal anatomy of glenohumeral ligaments. Figure also shows origination of SGHL from anterior supraglenoid tubercle. **B.** Drawing shows origination of SGHL from posterior supraglenoid tubercle. **C.** Drawing shows SGHL originating with LHBT. **D-F.** Drawings show types of conjugation of SGHL with MGHL. AB-IGHL = anterior band of inferior glenohumeral ligament, BT = long head of biceps tendon, IST = infraspinatus tendon, MGHL = middle glenohumeral ligament, PB-IGHL = posterior band of inferior glenohumeral ligament, SGHL = superior glenohumeral ligament, SSC = subscapularis tendon, SST = supraspinatus tendon, TM = teres minor tendon

arthrography. The glenoid labrum deepens and increases the surface area of the articulation (13). It also serves as a primary anchoring structure for the GHLs, the capsule, and the LHBT (3). Superiorly, the glenoid labrum blends with the SGHL and the LHBT; and anteriorly, it blends with the anterior band of the IGHL (14).

The rotator interval consists of the following structures, in the order from outside to inside: the coracohumeral ligament (CHL), the interval capsule, and the SGHL. The rotator interval capsule is reinforced by the CHL and the SGHL. The CHL arises from the dorsolateral aspect of the base of the coracoid process and courses through the rotator interval to blend with fibers from the SGHL. Its fibers then attach laterally to the greater tuberosity, fusing with the anterior fibers of the supraspinatus tendon insertion and the medial bicipital sheath, before fusing with the superior fibers of the subscapularis tendon insertion (13).

The rotator interval may be thought of as a roof over the intraarticular portion of the LHBT (3) which arises from the anterosuperior labrum (13, 14). The CHL and SGHL are composed of a sling-like band surrounding the LHBT proximal to the bicipital sulcus (13).

The SGHL is a focally thickened band in the glenohumeral joint capsule. It originates from the supraglenoid tubercle anterior to the LHBT attachment, and inserts into the fovea capitis line superior to the lesser tuberosity of the bicipital

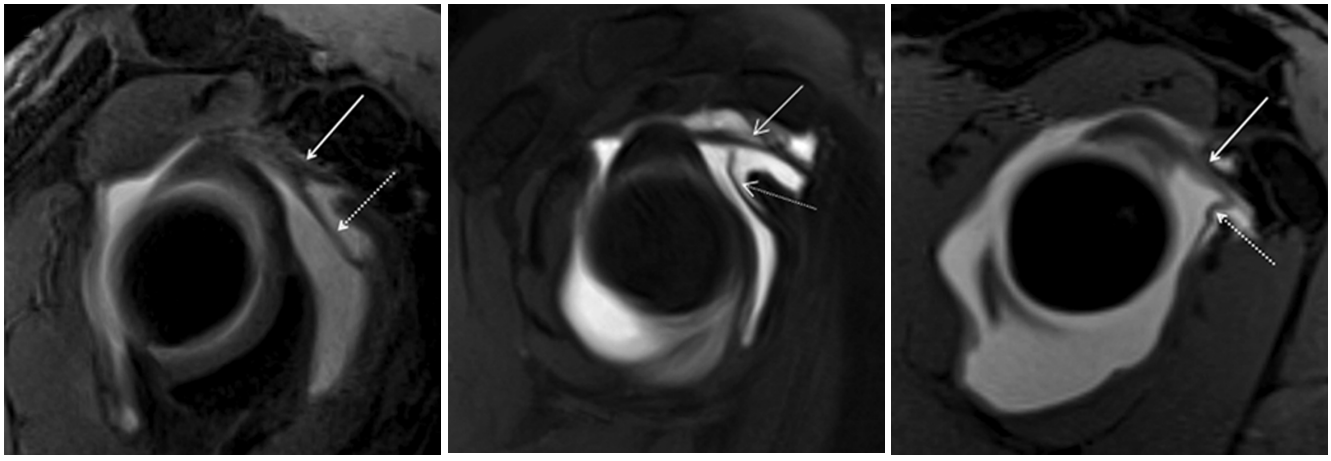

A B C

Fig. 5. Types of conjugation of SGHL with MGHL in three different patients.
A. Oblique sagittal fat-saturated 3D VIBE MR arthrographic image shows distal conjugation of SGHL (white arrow) with MGHL (white dotted arrow). **B.** Oblique sagittal fat-saturated 3D VIBE MR arthrographic image shows conjugation in mid segment of SGHL (white arrow) with MGHL (white dotted arrow). **C.** Oblique sagittal fat-saturated 3D VIBE MR arthrographic image shows proximal conjugation of SGHL (white arrow) with MGHL (white dotted arrow). MGHL = middle glenohumeral ligament, SGHL = superior glenohumeral ligament, 3D VIBE = three-dimensional volumetric interpolated breath-hold examination

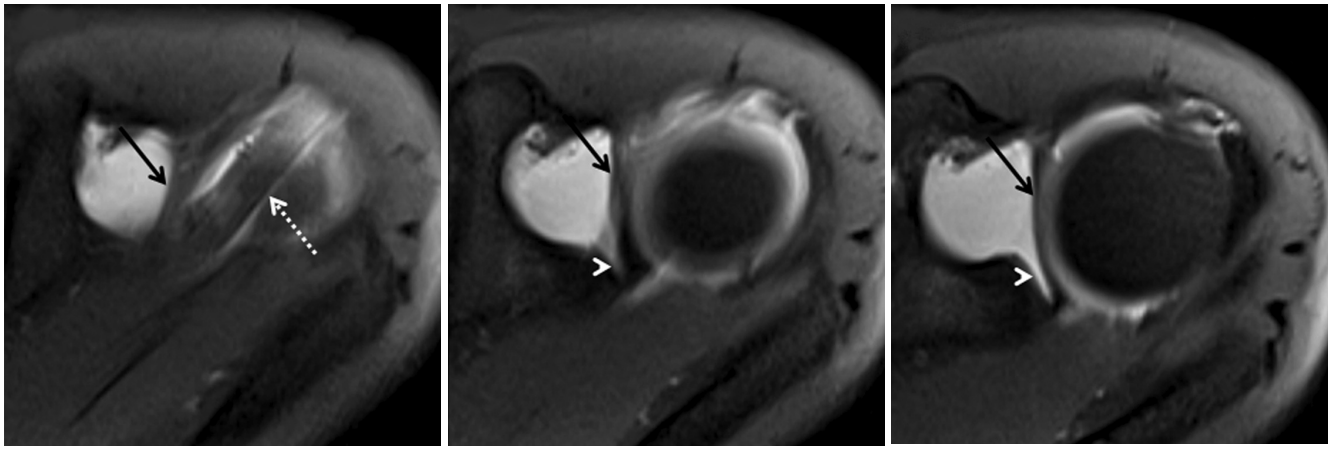

Fig. 6. Origination from posterior supraglenoid tubercle of SGHL with LHBT, in 32-year-old woman who suffered from shoulder pain. Consecutive axial fat-saturated T1-weighted MR arthrographic images show origination of SGHL (black arrow) with LHBT (white dotted arrow) from posterior supraglenoid tubercle. Linear focus of contrast material extending into sublabral sulcus (white arrowhead) is noted. LHBT = long head of biceps tendon, SGHL = superior glenohumeral ligament

Korean Journal of Radiology
KJR

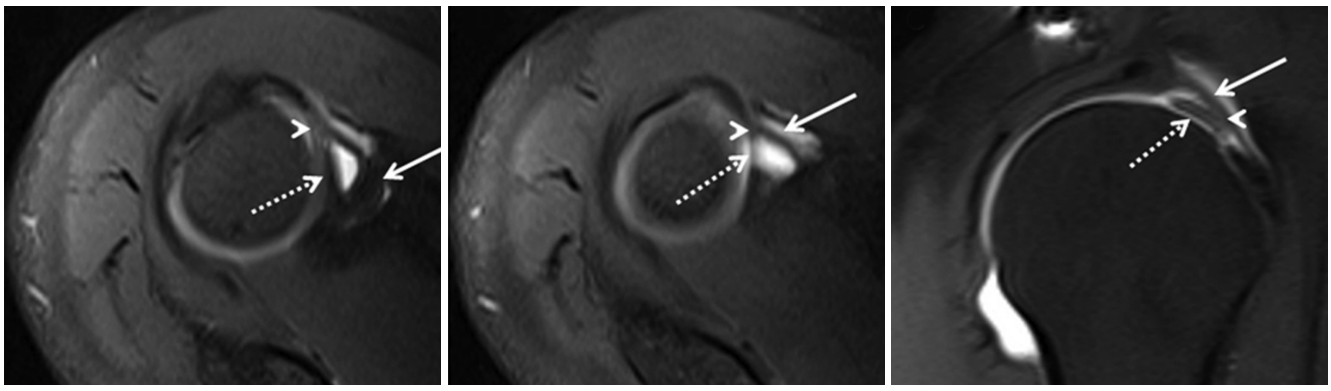

Fig. 7. Origination of SGHL from both anterior supraglenoid tubercle and LHBT, in 29-year-old woman who suffered from shoulder pain.
A, B. Consecutive axial fat-saturated T1-weighted MR arthrographic images show origination (white arrowhead) of SGHL (white arrow) from both anterior supraglenoid tubercle and LHBT (white dotted arrow). **C.** Oblique sagittal T1-weighted MR arthrographic image shows fan-shaped insertion (white arrowhead) of SGHL (white arrow) into LHBT (white dotted arrow). LHBT = long head of biceps tendon, SGHL = superior glenohumeral ligament

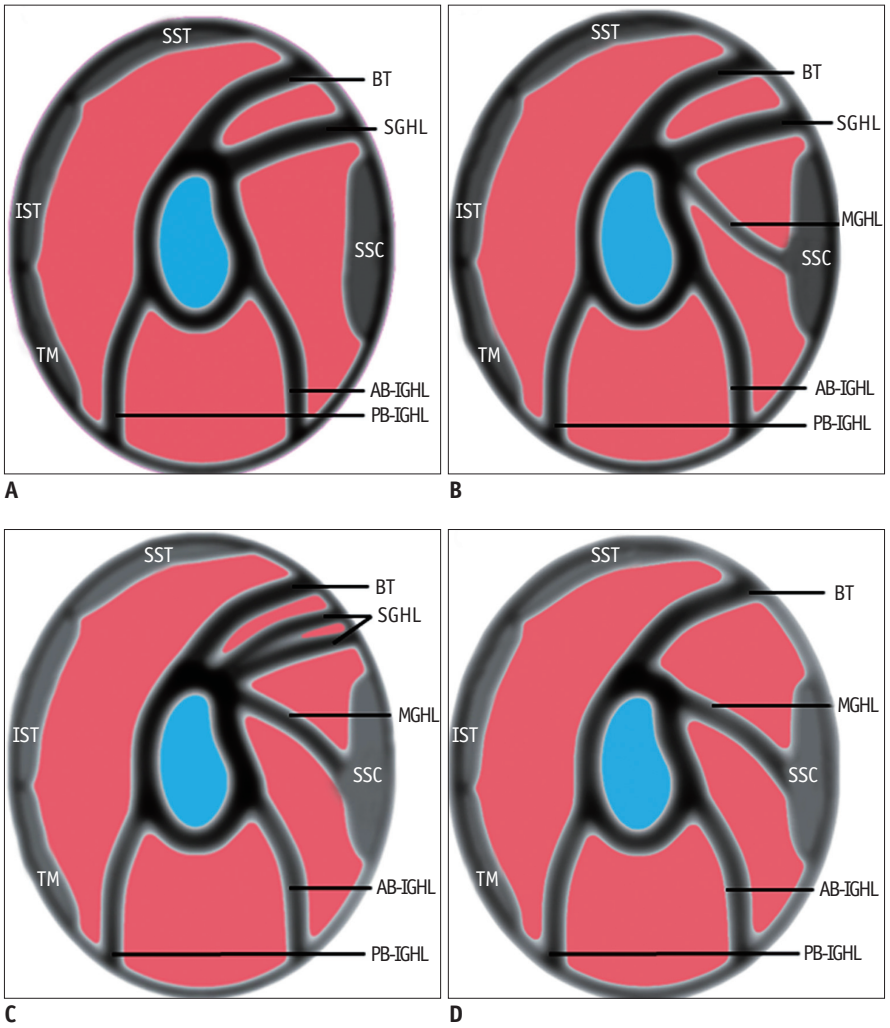

Fig. 8. Types of variations in shape and size of SGHL.
A. Drawing (lateral view) shows thick SGHL and absent MGHL. **B.** Drawing shows thick SGHL and thin MGHL. **C.** Drawing shows double SGHL. **D.** Drawing shows absent SGHL. AB-IGHL = anterior band of inferior glenohumeral ligament, BT = long head of biceps tendon, IST = infraspinatus tendon, MGHL = middle glenohumeral ligament, PB-IGHL = posterior band of inferior glenohumeral ligament, SGHL = superior glenohumeral ligament, SSC = subscapularis tendon, SST = supraspinatus tendon, TM = teres minor tendon

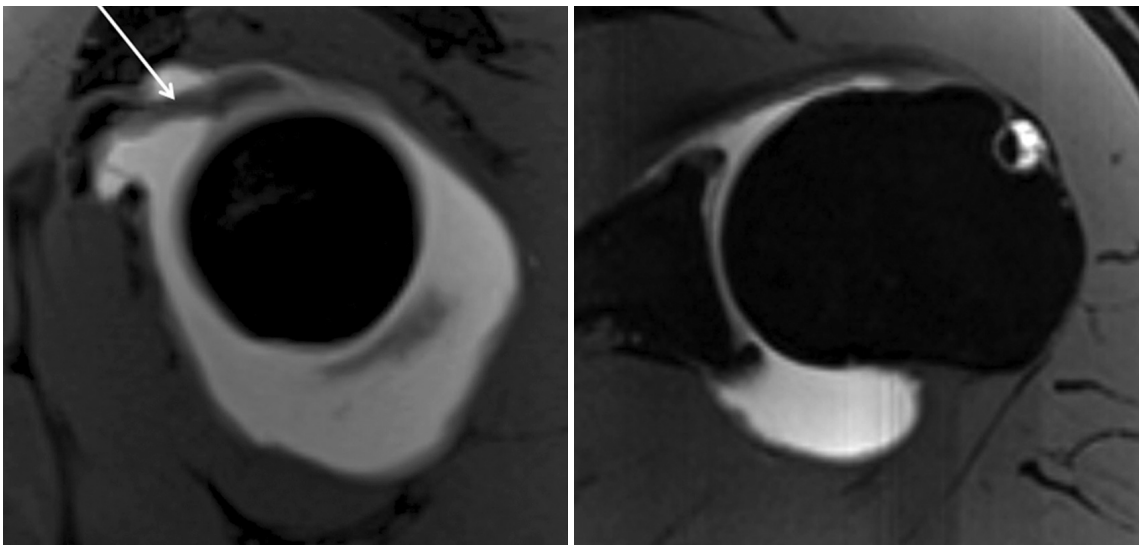

Fig. 9. Thick SGHL and absence of MGHL in 47-year-old woman who suffered from chronic shoulder pain. Oblique sagittal and axial fat-saturated 3D VIBE MR arthrographic images showing thick SGHL (white arrow) and absence of MGHL. MGHL = middle glenohumeral ligament, SGHL = superior glenohumeral ligament, 3D VIBE = three-dimensional volumetric interpolated breath-hold examination

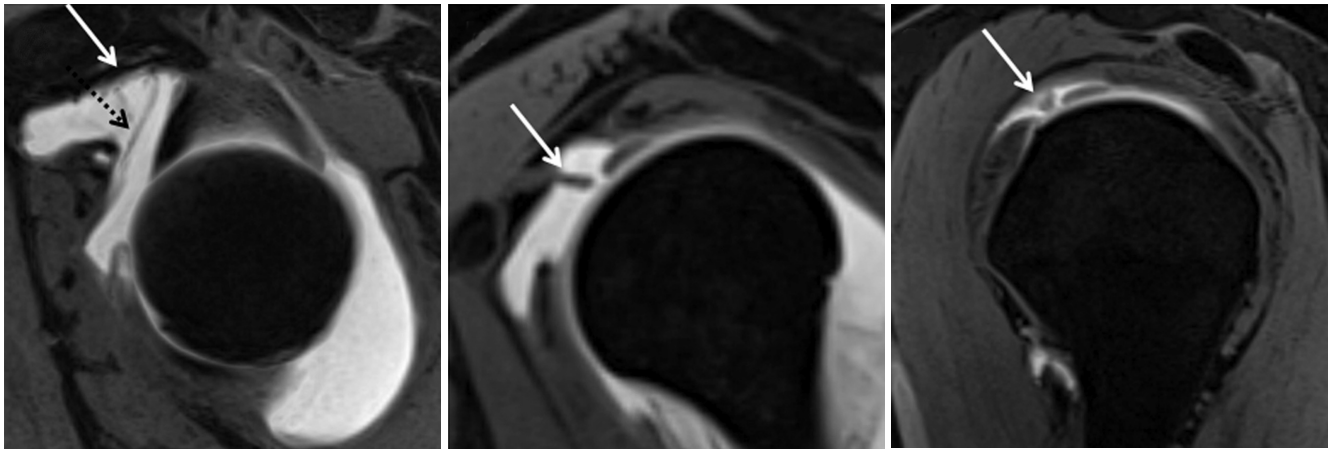

Fig. 10. Thick SGHL and thin MGHL in 43-year-old man who suffered from shoulder pain. Consecutive oblique sagittal fat-saturated 3D VIBE MR arthrographic images show thick SGHL (white arrow) and thin MGHL (black dotted arrow). MGHL = middle glenohumeral ligament, SGHL = superior glenohumeral ligament, 3D VIBE = three-dimensional volumetric interpolated breath-hold examination

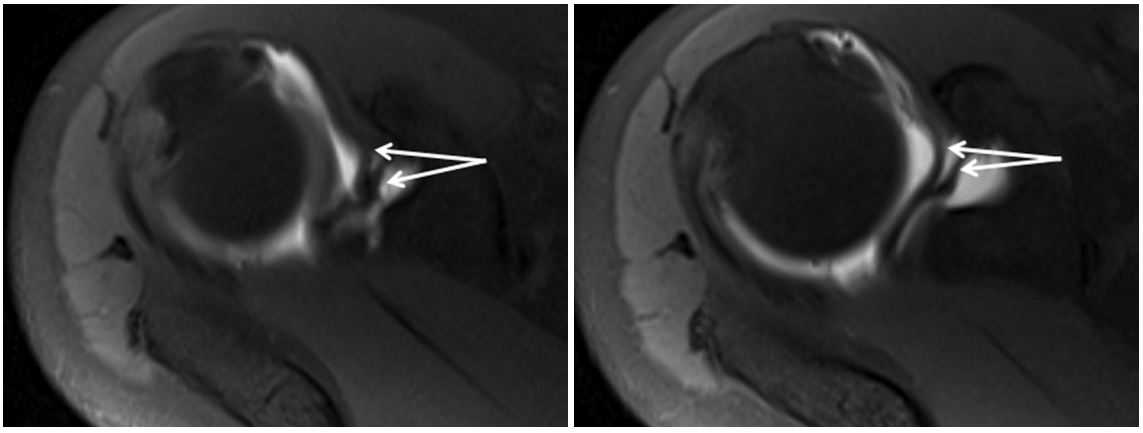

Fig. 11. Double SGHL in 31-year-old woman who suffered from shoulder pain. Consecutive axial fat-saturated T1-weighted MR arthrographic images show double SGHL (white arrows). SGHL = superior glenohumeral ligament

Korean Journal of Radiology
KJR

sulcus (13, 15). Thus, it contributes to the biceps pulley.

The SGHL is identified in 97–98% of the patients through arthroscopic and arthrographic series (16). Macroscopically, the SGHL is U-shaped and this shape lends support to the LHBT in the superior aspect of the bicipital sulcus (13). The SGHL runs parallel to the coracoid process and nearly perpendicular to the MGHL (1, 3, 13, 14, 16).

Using MR arthrography, the SGHL is best visualized in the sagittal oblique and axial planes (Fig. 3). In the axial plane, the SGHL is visualized as a low signal intensity intraarticular structure parallel to the coracoid process. Sagittal oblique MR arthrography shows that the SGHL is located underneath the coracoid process and CHL. A normal foramen exists between the SGHL and the MGHL, allowing communication of the glenohumeral joint cavity through the subscapularis recess (1, 3, 17, 18).

Congenital Variants of the Superior Glenohumeral Ligament

The SGHL usually originates from the supraglenoid tubercle, just anterior to the LHBT attachment. However, its origin may vary (posterior supraglenoid tubercle, superior labrum, LHBT, MGHL, or some combination) (Figs. 4-7)

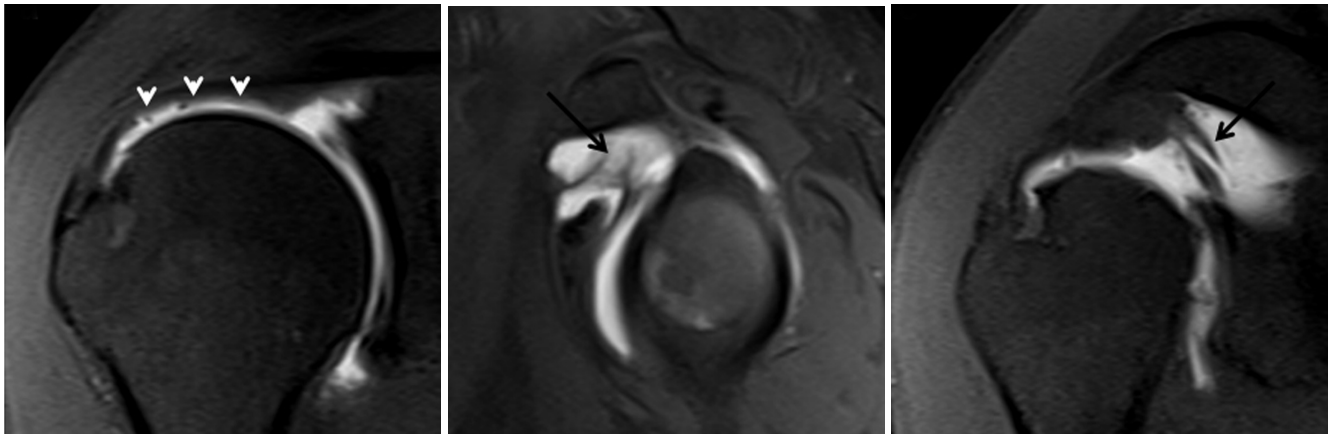

A B C

Fig. 12. Partial tear of undersurface of supraspinatus tendon with SGHL tear in 47-year-old man.
A. Oblique coronal fat-saturated T1-weighted MR arthrographic image shows partial tear of undersurface of supraspinatus tendon (white arrowheads). **B, C.** Oblique sagittal and oblique coronal fat-saturated T1-weighted MR arthrographic images show SGHL tear (black arrow). SGHL = superior glenohumeral ligament

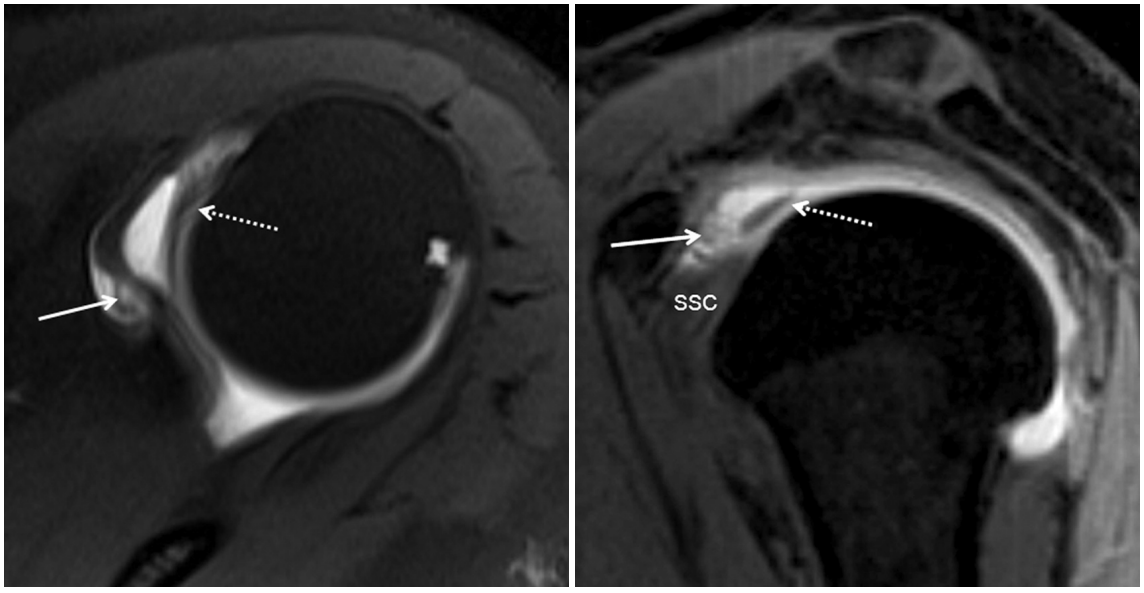

Fig. 13. Habermeyer group 1 lesion in 45-year-old man. Axial fat-saturated T1-weighted and oblique sagittal fat-saturated 3D VIBE MR arthrographic images show isolated superior GHL tear (white arrow). White dotted arrow = LHBT. GHL = glenohumeral ligament, LHBT = long head of biceps tendon, SSC = subscapularis tendon, 3D VIBE = three-dimensional volumetric interpolated breath-hold examination

(17, 19). Although the SGHL may vary in shape and size (Fig. 8), it usually presents as a thick structure when the MGHL is absent or undeveloped (Figs. 9, 10) (16, 18-20). The SGHL is consistently identified as capsular ligament by MR arthrography and arthroscopy examination. It may be absent in arthroscopic and MR arthrographic series, in 2–3% of the patients (16). In a recent study by Kask et al. (20), the SGHL was found in all 27 shoulder joint specimens investigated. A longitudinal split or duplicate ligament may reflect a normal variant or a longitudinal tear of the SGHL (Fig. 11).

Pathologies of the Superior Glenohumeral Ligament

Magnetic resonance arthrography of the glenohumeral joint is the most accurate imaging technique established, for identifying pathologies of the SGHL and the associated

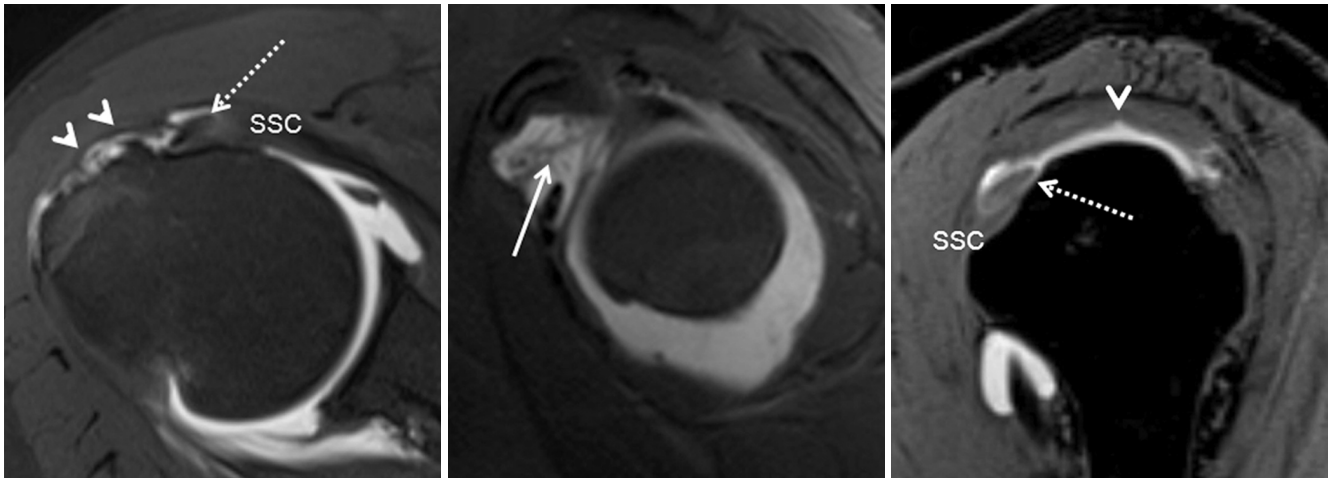

A B C

Fig. 14. Habermeyer group 2 lesion in 47-year-old woman.
A. Axial fat-saturated T1-weighted MR arthrographic image shows partial articular-side supraspinatus tendon tear (white arrowheads). LHBT is slightly dislocated anteriorly (white dotted arrow). **B.** Oblique sagittal fat-saturated T1-weighted MR arthrographic image demonstrates fraying of SGHL (white arrow). **C.** Oblique sagittal fat-saturated 3D VIBE MR arthrographic image demonstrates displacement sign. LHBT (white dotted arrow) shows contact with superior border of intact subscapularis tendon (SSC) on midsection through lesser tuberosity. SGHL is invisible. Image also shows partial tear on articular-side supraspinatus tendon (white arrowhead), increased signal intensity, and diameter of LHBT (white dotted arrow). LHBT = long head of biceps tendon, SGHL = superior glenohumeral ligament, 3D VIBE = three-dimensional volumetric interpolated breath-hold examination

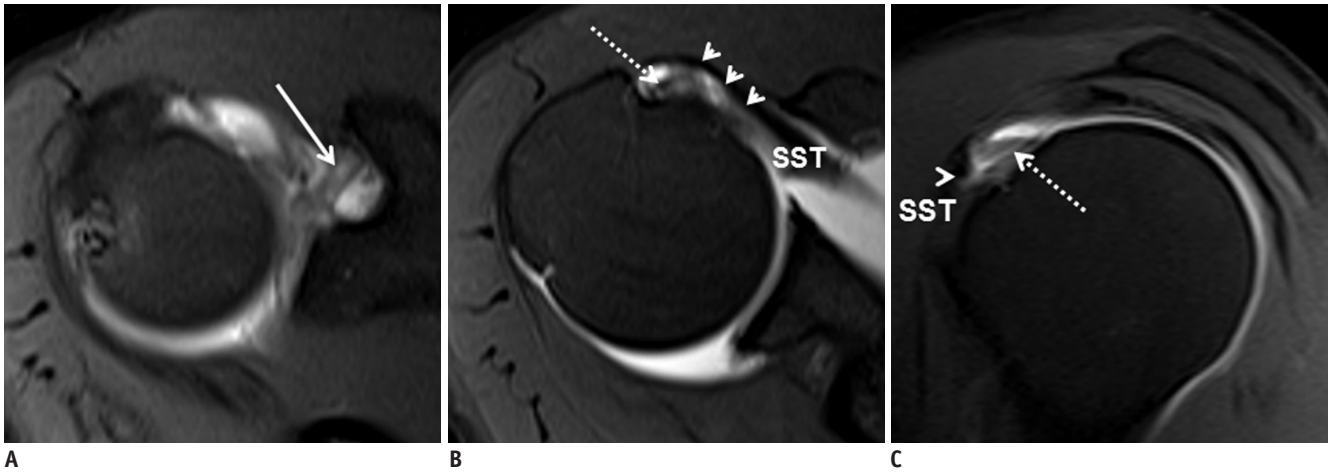

A B C

Fig. 15. Habermeyer group 3 lesion in 38-year-old woman.
A, B. Consecutive axial fat-saturated T1-weighted MR arthrographic images show superior GHL lesion (white arrow) with partial tear on articular-side of subscapularis tendon (white arrowheads). LHBT (white dotted arrow) shows slight medial subluxation. **C.** Oblique sagittal fat-saturated T1-weighted MR arthrographic image shows contrast agent entering defect (arrowhead) of superior subscapularis tendon (SSC), consistent with partial tear. LHBT (white dotted arrow) shows contact with superior border of SSC on midsection through lesser tuberosity. LHBT = long head of biceps tendon, SST = supraspinatus tendon

Korean Journal of Radiology
KJR

structures. In a retrospective study comparing MR arthrographic findings with surgical findings, Chandnani et al. (21) determined that MR arthrography had a sensitivity of 100%, a specificity of 94%, and an accuracy of 94% in the diagnosis of SGHL tears. A torn SGHL may be observed in MR arthrography images as increased signal intensity that looks like disruptions and thick, wavy, or irregular structures (19, 22).

The biceps pulley is an important component of the rotator interval. This complex anatomical structure

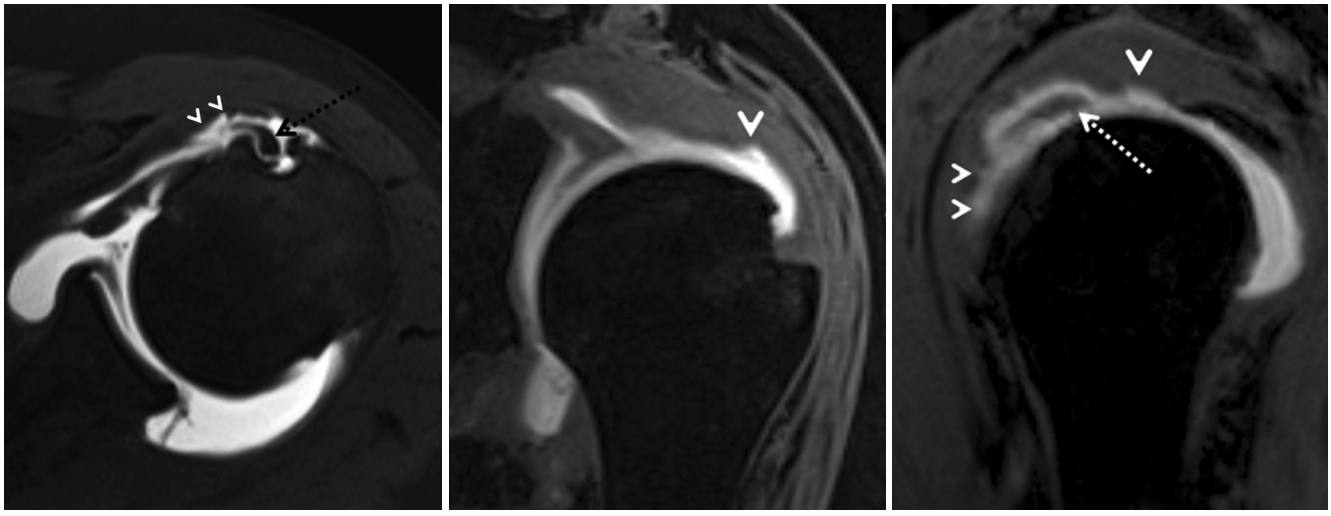

Fig. 16. Habermeyer group 4 lesion in 55-year-old man.
A. Axial fat-saturated T1-weighted MR arthrographic image shows medial subluxation of LHBT (black dotted arrow) with partial tear on articular-side of subscapularis tendon (white arrowheads). **B.** Oblique coronal fat-saturated 3D VIBE MR arthrographic image shows partial tear on articular-side of supraspinatus tendon (white arrowhead). **C.** Oblique sagittal fat-saturated 3D VIBE MR arthrographic image shows partial tears on articular-side of supraspinatus and subscapularis tendons. Displacement sign is shown, with LHBT (white dotted arrow) cutting into superior portion of subscapularis tendon (small white arrowheads). Image also shows partial tear on articular-side of supraspinatus tendon (big white arrowhead), increased signal intensity, and diameter of LHBT (white dotted arrow). LHBT = long head of biceps tendon, 3D VIBE = three-dimensional volumetric interpolated breath-hold examination

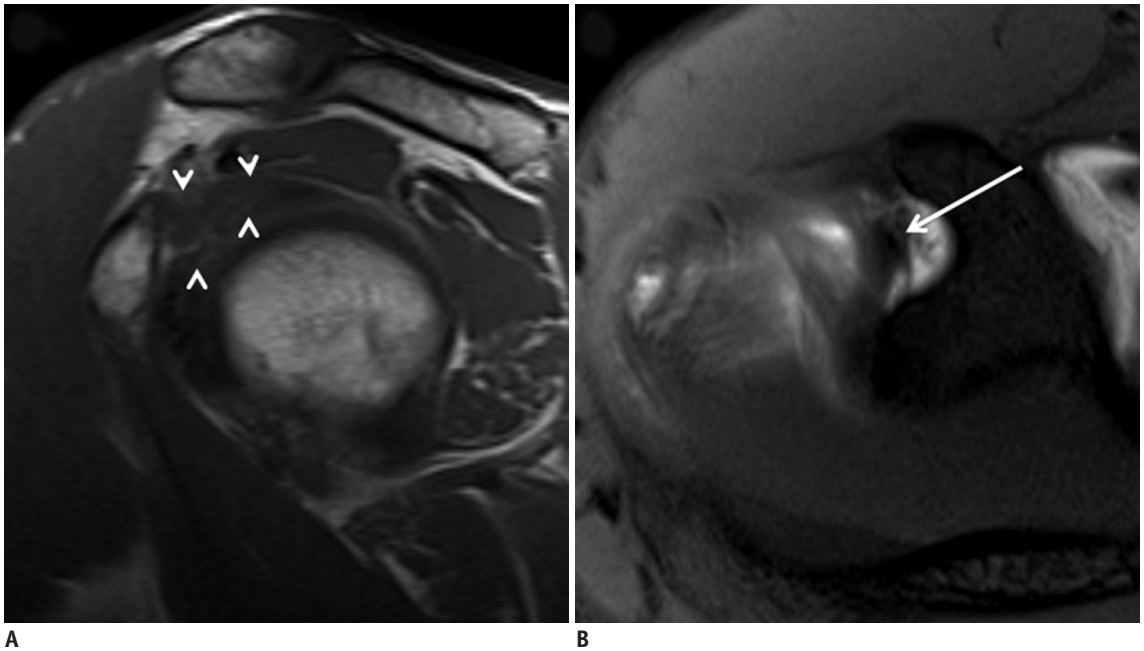

Fig. 17. Frozen shoulder of 45-year-old man.
A. Oblique sagittal T1-weighted MR image shows complete obliteration of subcoracoid fat triangle (white arrowheads). **B.** Axial fat-saturated T1-weighted MR arthrographic image shows thickened SGHL (white arrow). SGHL = superior glenohumeral ligament

consists of the SGHL and the CHL, and it is also in direct contact with the distal fibers of the subscapularis and the supraspinatus tendons. Based on this complex relationship, it has been suggested that the SGHL is the major stabilizing component in the anterosuperior portion of the glenohumeral joint capsule (23-27). It prevents dislocation of the LHBT in the intraarticular course. Therefore, tears in this ligament may lead to medial subluxation or dislocation of the LHBT. Recently, Schaeffeler et al. (28) showed that the prevalence of isolated SGHL tears is 29%.

Biceps pulley lesions can occur due to acute trauma, degenerative changes, repetitive microtrauma, congenital rotator interval defects, or injuries associated with tear in a rotator cuff (13, 24, 28-30). These lesions are thought to be responsible for medial subluxation of the LHBT, and they may result in loss of function in the shoulder and pain in the anterior shoulder (24, 25, 31).

Lesions of the biceps pulley are common in the patients undergoing arthroscopic shoulder surgery. The frequency of lesions on isolated biceps pulley is 29–74% (24, 25, 28). A recent study by Braun et al. (25) prospectively analyzed the prevalence of pulley lesions, which was reported as 32%,

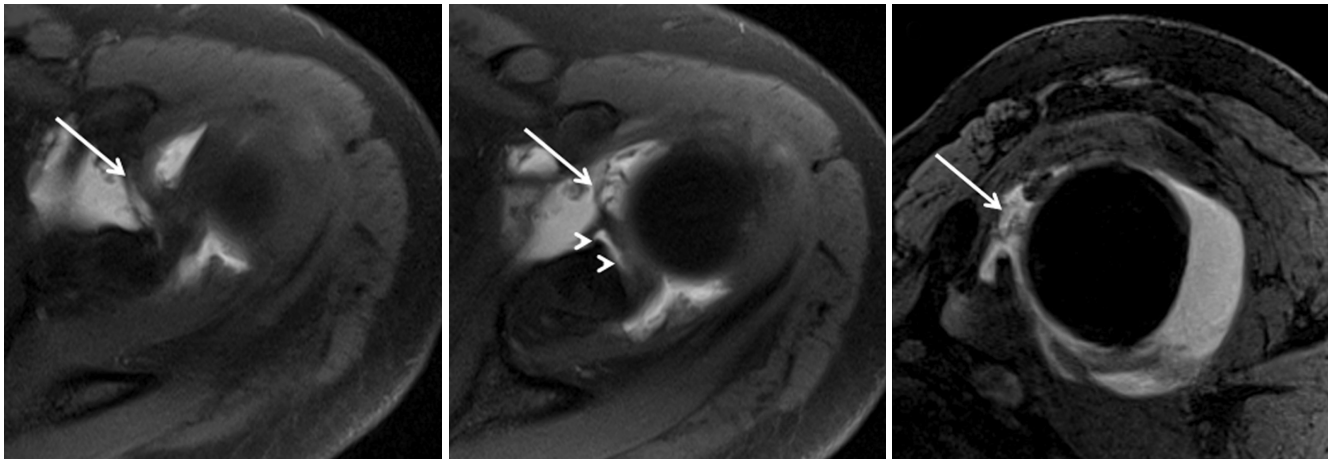

A B C

Fig. 18. Type X SLAP lesion with SGHL tear in 43-year-old man.
A, B. Consecutive axial fat-saturated 3D VIBE MR arthrographic images show tears of SGHL (white arrow) and superior labrum (white arrowheads). **C.** Oblique sagittal fat-saturated 3D VIBE MR arthrographic image shows SGHL tear (white arrow) between subscapularis tendon and LHBT. LHBT = long head of biceps tendon, SGHL = superior glenohumeral ligament, SLAP = superior labrum anterior and posterior, 3D VIBE = three-dimensional volumetric interpolated breath-hold examination

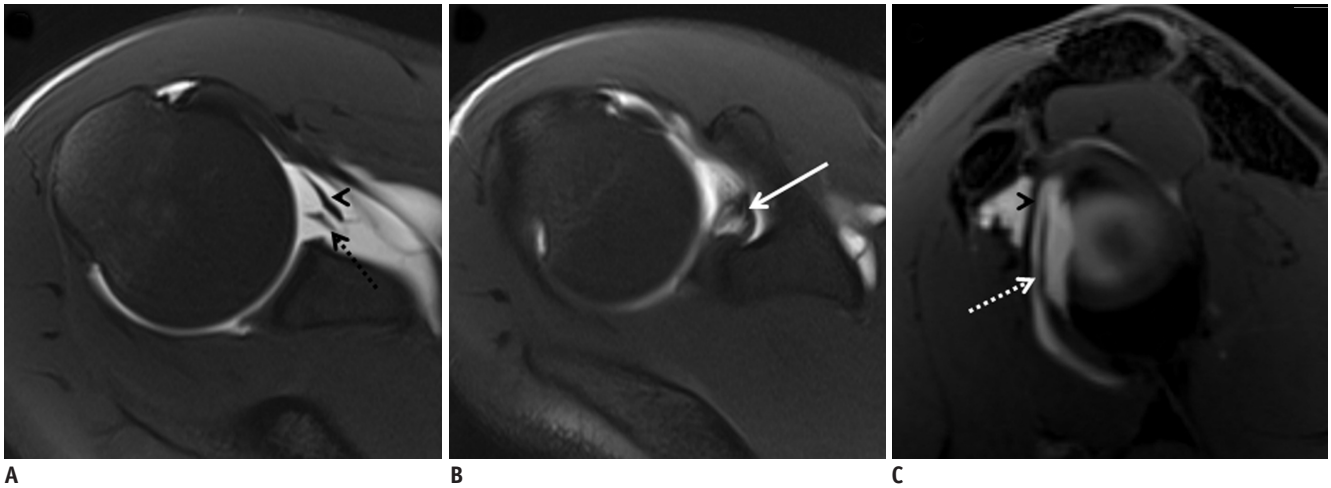

A B C

Fig. 19. Massive anterior labral tear with SGHL tear in 36-year-old man.
A. Axial fat-saturated T1-weighted MR arthrographic image shows avulsion of anteroinferior glenoid labrum (black dotted arrow) behind MGHL (black arrowhead). **B.** Upper section of axial fat-saturated T1-weighted MR arthrography shows SGHL tear (white arrow). **C.** Oblique sagittal fat-saturated 3D VIBE MR arthrographic image shows massive avulsion of anterior glenoid labrum (white dotted arrow) behind MGHL (black arrowhead). MGHL = middle glenohumeral ligament, SGHL = superior glenohumeral ligament, 3D VIBE = three-dimensional volumetric interpolated breath-hold examination

Korean Journal of Radiology
KJR

in a consecutive series of patients undergoing arthroscopic shoulder surgery. In this study, tears in the pulley complex were present in 67 of 207 shoulders. Weishaupt et al. (23) reported discontinuity of the SGHL in biceps pulley lesions. The lesions of the biceps pulley, the LHBT, the subscapularis, and the supraspinatus tendon are often closely associated with each other (Fig. 12) (25). The instability pattern of the LHBT and the presence of tears on the rotator cuff tendons adjacent to the rotator interval can be used to diagnose biceps pulley lesions. Walch et al. (31) investigated the rotator interval in a series of 116 patients with isolated lesions of the supraspinatus tendon. Lesion in the biceps pulley and millimetric tears on the superior border of the subscapularis tendon occurred

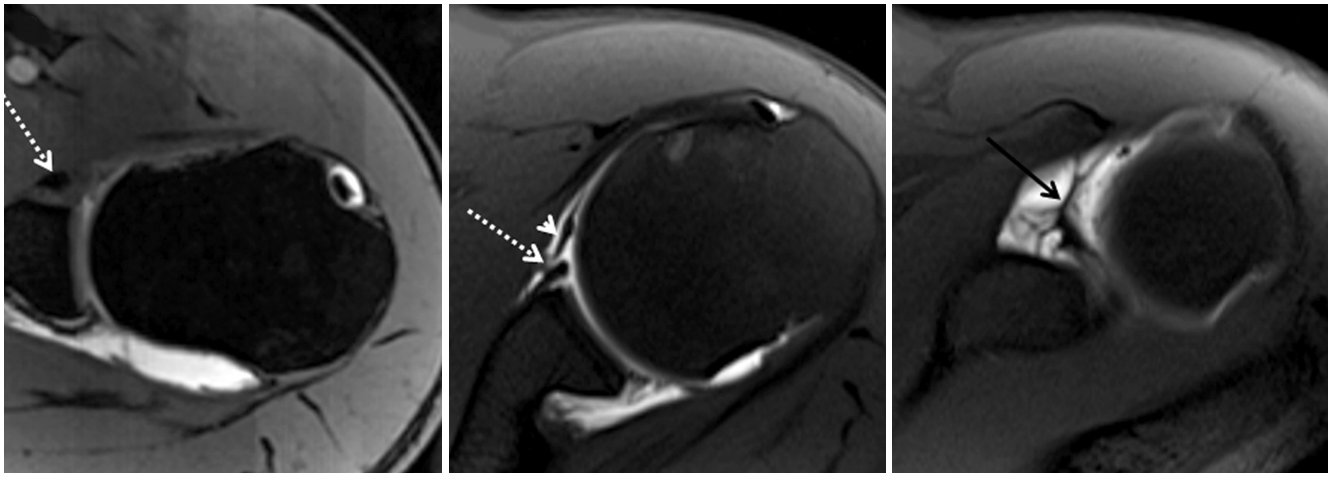

Fig. 20. Bony Bankart lesion with SGHL tear in 38-year-old woman who suffered from recurrent shoulder dislocations.
A. Axial fat-saturated 3D VIBE MR arthrographic image shows classic bony Bankart lesion, with avulsion of anteroinferior glenoid bone and labrum (white dotted arrow). **B.** Upper section of axial fat-saturated T1-weighted MR arthrography shows avulsion of anterior glenoid labrum (white dotted arrow) behind MGHL (white arrowhead). **C.** Axial fat-saturated T1-weighted MR arthrographic image at level of coracoid process shows SGHL tear (black arrow). MGHL = middle glenohumeral ligament, SGHL = superior glenohumeral ligament, 3D VIBE = three-dimensional volumetric interpolated breath-hold examination

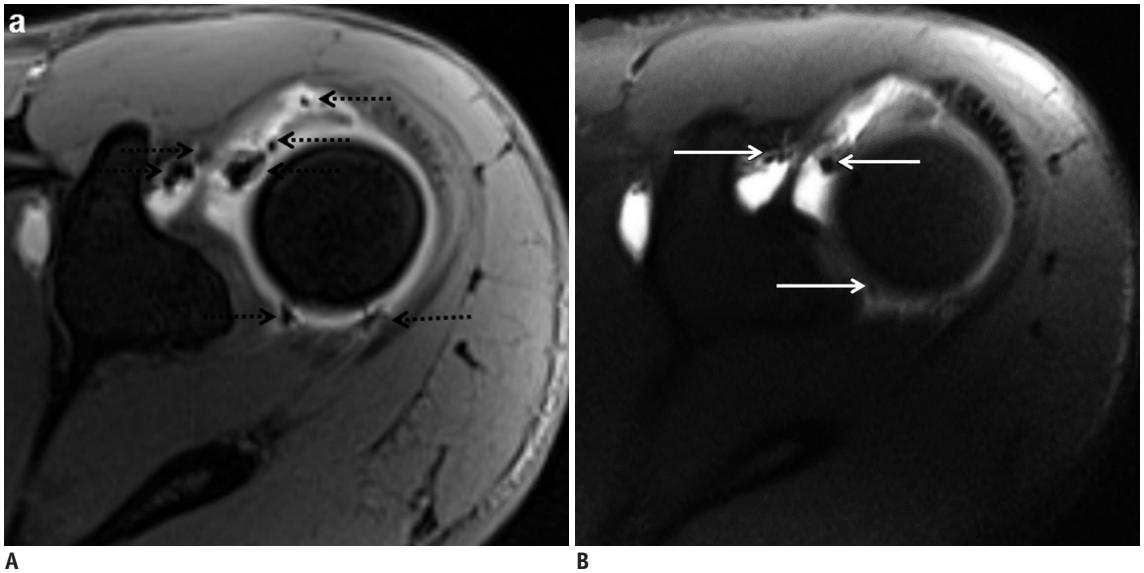

Fig. 21. Susceptibility artifacts caused by inadvertently injected air in 47-year-old man who suffered from anterosuperior shoulder pain.
A. Axial fat-saturated 3D VIBE MR arthrographic image shows small air bubbles (black dotted arrows) distributed at superior part of joint cavity. Susceptibility artifacts may be more pronounced in VIBE MR arthrographic images. **B.** Axial fat-saturated T1-weighted MR arthrographic image at same level as VIBE sequence shows smaller air bubbles (white arrows) distributed at superior part of joint cavity. 3D VIBE = three-dimensional volumetric interpolated breath-hold examination

in 19 of 116 shoulders. A recent arthrographic study by Schaeffeler et al. (28) concluded that the presence of associated tendinopathy of the LHBT in oblique sagittal MR arthrography images has additional value for the diagnosis of a pulley lesion.

Biceps pulley lesions are difficult to diagnose by routine arthroscopic examination, so they are called "hidden lesions". These injuries have been arthroscopically classified by Bennett (32), and this arthroscopic classification system is based on lesions involving the SGHL, the CHL, and the subscapularis tendon; however, it is not applicable for MR arthrography (28). Habermeyer et al. (24) subsequently classified biceps pulley lesions into four different patterns, which shows the importance of the SGHL in the lateral rotator interval (28, 31). According to the Habermeyer classification system, Group 1 lesions represent the isolated tears in SGHL, with the subscapularis and supraspinatus tendons intact without biceps tendon instability (Fig. 13). Group 2 lesions involve a biceps pulley lesion in association with a partial tear in the articular-side supraspinatus tendon and a mild medial subluxation of the LHBT (Fig. 14). Group 3 lesions involve a biceps pulley lesion in association with a partial tear on articular-side subscapularis tendon and a subluxation of the LHBT (Fig. 15). Group 4 lesions involve a biceps pulley lesion in association with partial tears on articular-side of both the supraspinatus and subscapularis tendons and a medial dislocation of the LHBT (Fig. 16).

The diseases associated with biceps pulley lesions include internal anterosuperior impingement, instability of the LHBT, biceps tendinopathy, superior labrum anterior and posterior lesions (SLAP), and adhesive capsulitis (13). The SGHL can be thicker in the patients with adhesive capsulitis (Fig. 17) (17). Internal anterosuperior impingement was first described by Gerber and Sebesta (33) as a form of intraarticular impingement responsible for unexplained anterior shoulder pain. Habermeyer et al. (24) subsequently described this disease as an impingement of the LHBT by the anterosuperior glenoid rim. In an arthroscopic study, Habermeyer et al. (24) found partial tears on articular side of subscapularis tendon in 71.8% of the patients with anterosuperior impingement.

Superior labrum anterior and posterior lesions may be associated with lesions of the rotator interval and biceps pulley complex, and this was clearly described by Braun

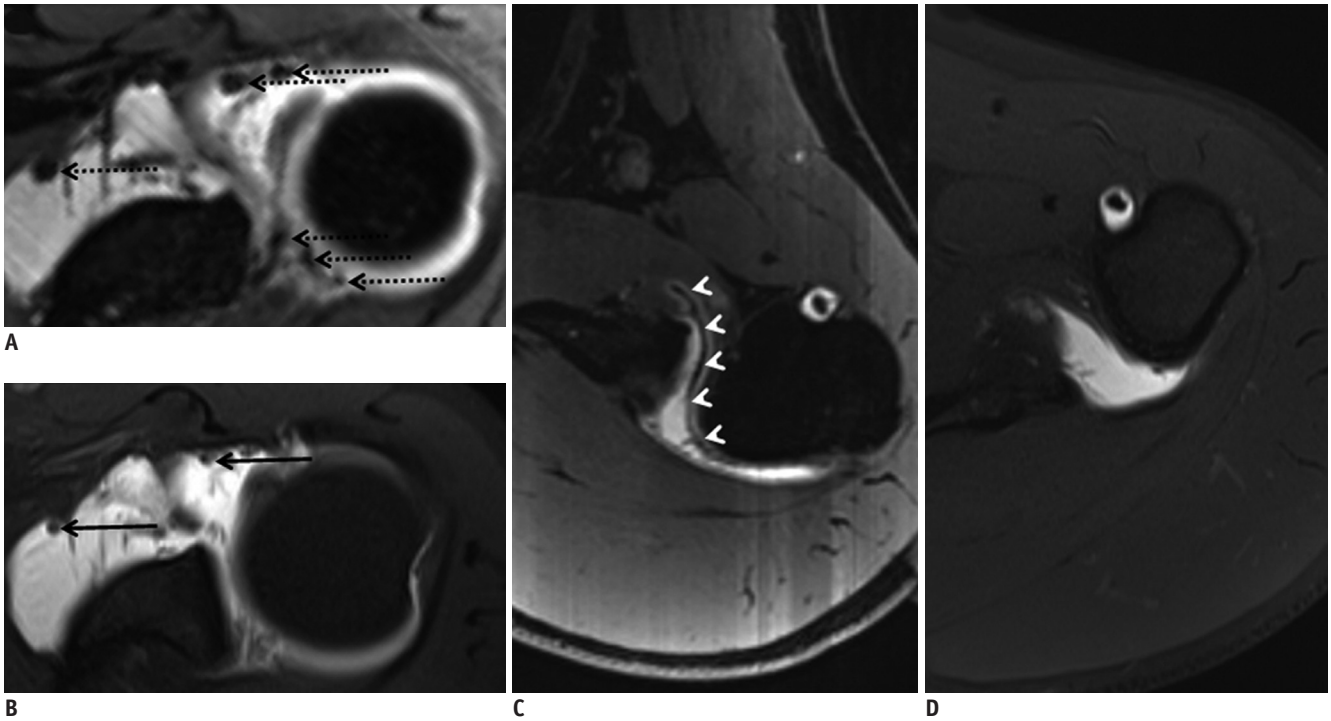

Fig. 22. Bony Bankart lesion with intraarticular blooming artifacts in 41-year-old man who suffered from shoulder dislocations. In this patient, hemosiderin deposits in synovium have been confirmed by arthroscopy.
A. Axial fat-saturated 3D VIBE MR arthrographic image at level of superior glenoid shows multiple blooming artifacts (black dotted arrows) at superior part of joint cavity. **B.** Axial fat-saturated T1-weighted MR arthrographic image at same level as **A** shows smaller blooming artifacts (black arrows). **C.** Axial fat-saturated 3D VIBE MR arthrographic image at level of axillary recess shows synovial haemosiderin deposits (white arrowheads). **D.** Axial fat-saturated T1-weighted MR arthrographic image at same level as **C** does not show evidence of synovial haemosiderin deposits.

Korean Journal of Radiology
KJR

et al. (25) in a recent arthroscopic study. Four types of SLAP lesions were classified by Snyder et al. (34) based on arthroscopic findings. This original classification system is still the most widely accepted one, and six additional classifications have been developed. These new classifications represent the combination of SLAP lesions, with extension into different areas of the glenoid labrum and other adjacent capsuloligamentous structures. According to the new classifications, a Type 10 lesion consists of a superior labral tear with extension into the rotator interval complex (Fig. 18) (13). Otherwise, in patients with shoulder instability, the extensive anterior and anterosuperior labral tears can extend into the SGHL and MGHL (Figs. 19, 20) (19).

Diagnostic Pitfalls

Magnetic resonance arthrography of the glenohumeral joint is sensitive to susceptibility artifacts caused by inadvertently injected intraarticular air bubbles. With advanced sequences, such as fat-suppressed VIBE, even small amounts of air bubbles may produce pronounced susceptibility artifacts (35). Air tends to be located in the uppermost parts of the glenohumeral joint. Therefore, small air bubbles are usually distributed at the anterosuperior part of the joint cavity, next to the SGHL or CHL and the horizontal part of the LHBT (Fig. 21) (35, 36). Air bubbles may occasionally mimic intraarticular loose bodies, chondrocalcinosis of hyaline cartilage, and inflammatory adhesions of the joint capsule. Knowledge of the intraarticular arrangement of gas bubbles would help in avoiding misinterpretation (36).

Haemorrhagic effusion is usually an expected complication after dislocation of the glenohumeral joint. The haemorrhage resolves over time, but the hemosiderin particles may accumulate in the synovium. These particles are usually not visualized by the routine sequences. Concordantly, the VIBE sequence is a sensitive technique that will reveal the hemosiderin particles in the synovium and joint space, as well as intra-articular air bubbles (Fig. 22).

CONCLUSIONS

The SGHL is known to be difficult to evaluate based on anatomical structures identified in arthrographic and arthroscopic examinations. The assessment of the SGHL is important for the diagnosis of biceps pulley lesions. The SGHL can be ruptured as an isolated form and it can also be damaged with anterosuperior impingement syndrome, biceps tendon instability, SLAP lesions, and anterior instability of the glenohumeral joint. In addition to routine MR arthrography sequences, advanced MR arthrographic sequences such as VIBE may greatly help in the diagnosis of the SGHL and in identifying its morphology and the associated pathologies.

REFERENCES

1. Bencardino JT, Beltran J. MR imaging of the glenohumeral ligaments. *Magn Reson Imaging Clin N Am* 2004;12:11-24, v
2. Yang C, Goto A, Sahara W, Yoshikawa H, Sugamoto K. In vivo three-dimensional evaluation of the functional length of glenohumeral ligaments. *Clin Biomech (Bristol, Avon)* 2010;25:137-141
3. Robinson G, Ho Y, Finlay K, Friedman L, Harish S. Normal anatomy and common labral lesions at MR arthrography of the shoulder. *Clin Radiol* 2006;61:805-821
4. Cooper DE, O'Brien SJ, Warren RF. Supporting layers of the glenohumeral joint. An anatomic study. *Clin Orthop Relat Res* 1993;(289):144-155
5. Pouliart N, Somers K, Eid S, Gagey O. Variations in the superior capsuloligamentous complex and description of a new ligament. *J Shoulder Elbow Surg* 2007;16:821-836
6. Ogul H, Bayraktutan U, Yildirim OS, Suma S, Ozgokce M, Okur A, et al. Magnetic Resonance Arthrography of the Glenohumeral Joint: Ultrasonography-Guided Technique Using a Posterior Approach. *Eurasian J Med* 2012;44:73-78
7. Zwar RB, Read JW, Noakes JB. Sonographically guided glenohumeral joint injection. *AJR Am J Roentgenol* 2004;183:48-50
8. Souza PM, Aguiar RO, Marchiori E, Bardoe SA. Arthrography of the shoulder: a modified ultrasound guided technique of joint injection at the rotator interval. *Eur J Radiol* 2010;74:e29-e32
9. Yeh L, Kwak S, Kim YS, Pedowitz R, Trudell D, Muhle C, et al. Anterior labroligamentous structures of the glenohumeral joint: correlation of MR arthrography and anatomic dissection in cadavers. *AJR Am J Roentgenol* 1998;171:1229-1236
10. Flannigan B, Kursunoglu-Brahme S, Snyder S, Karzel R, Del Pizzo W, Resnick D. MR arthrography of the shoulder: comparison with conventional MR imaging. *AJR Am J Roentgenol* 1990;155:829-832
11. Kaplan PA, Bryans KC, Davick JP, Otte M, Stinson WW, Dussault RG. MR imaging of the normal shoulder: variants and pitfalls. *Radiology* 1992;184:519-524
12. Chung CB, Dwek JR, Cho GJ, Lektrakul N, Trudell D, Resnick D. Rotator cuff interval: evaluation with MR imaging and MR arthrography of the shoulder in 32 cadavers. *J Comput Assist Tomogr* 2000;24:738-743
13. Nakata W, Katou S, Fujita A, Nakata M, Lefor AT, Sugimoto H. Biceps pulley: normal anatomy and associated lesions at MR

arthrography. *Radiographics* 2011;31:791-810
14. De Maeseneer M, Van Roy F, Lenchik L, Shahabpour M, Jacobson J, Ryu KN, et al. CT and MR arthrography of the normal and pathologic anterosuperior labrum and labral-bicipital complex. *Radiographics* 2000;20 Spec No:S67-S81
15. De Maeseneer M, Van Roy P, Shahabpour M. Normal MR imaging anatomy of the rotator cuff tendons, glenoid fossa, labrum, and ligaments of the shoulder. *Radiol Clin North Am* 2006;44:479-487, vii
16. Dunham KS, Bencardino JT, Rokito AS. Anatomic variants and pitfalls of the labrum, glenoid cartilage, and glenohumeral ligaments. *Magn Reson Imaging Clin N Am* 2012;20:213-228, x
17. Petchprapa CN, Beltran LS, Jazrawi LM, Kwon YW, Babb JS, Recht MP. The rotator interval: a review of anatomy, function, and normal and abnormal MRI appearance. *AJR Am J Roentgenol* 2010;195:567-576
18. Yu D, Turmezei TD, Kerslake RW. FIESTA: an MR arthrography celebration of shoulder joint anatomy, variants, and their mimics. *Clin Anat* 2013;26:213-227
19. Shankman S, Bencardino J, Beltran J. Glenohumeral instability: evaluation using MR arthrography of the shoulder. *Skeletal Radiol* 1999;28:365-382
20. Kask K, Põldoja E, Lont T, Norit R, Merila M, Busch LC, et al. Anatomy of the superior glenohumeral ligament. *J Shoulder Elbow Surg* 2010;19:908-916
21. Chandnani VP, Gagliardi JA, Murnane TG, Bradley YC, DeBerardino TA, Spaeth J, et al. Glenohumeral ligaments and shoulder capsular mechanism: evaluation with MR arthrography. *Radiology* 1995;196:27-32
22. Beltran J, Rosenberg ZS, Chandnani VP, Cuomo F, Beltran S, Rokito A. Glenohumeral instability: evaluation with MR arthrography. *Radiographics* 1997;17:657-673
23. Weishaupt D, Zanetti M, Tanner A, Gerber C, Hodler J. Lesions of the reflection pulley of the long biceps tendon. MR arthrographic findings. *Invest Radiol* 1999;34:463-469
24. Habermeyer P, Magosch P, Pritsch M, Scheibel MT, Lichtenberg S. Anterosuperior impingement of the shoulder as a result of pulley lesions: a prospective arthroscopic study. *J Shoulder Elbow Surg* 2004;13:5-12
25. Braun S, Horan MP, Elser F, Millett PJ. Lesions of the biceps pulley. *Am J Sports Med* 2011;39:790-795
26. Cooper DE, O'Brien SJ, Arnoczky SP, Warren RF. The structure and function of the coracohumeral ligament: an anatomic and microscopic study. *J Shoulder Elbow Surg* 1993;2:70-77
27. Werner A, Mueller T, Boehm D, Gohlke F. The stabilizing sling for the long head of the biceps tendon in the rotator cuff interval. A histoanatomic study. *Am J Sports Med* 2000;28:28-31
28. Schaeffeler C, Waldt S, Holzapfel K, Kirchhoff C, Jungmann PM, Wolf P, et al. Lesions of the biceps pulley: diagnostic accuracy of MR arthrography of the shoulder and evaluation of previously described and new diagnostic signs. *Radiology* 2012;264:504-513
29. Gaskill TR, Braun S, Millett PJ. Multimedia article. The rotator interval: pathology and management. *Arthroscopy* 2011;27:556-567
30. Baumann B, Genning K, Böhm D, Rolf O, Gohlke F. Arthroscopic prevalence of pulley lesions in 1007 consecutive patients. *J Shoulder Elbow Surg* 2008;17:14-20
31. Walch G, Nove-Josserand L, Levigne C, Renaud E. Tears of the supraspinatus tendon associated with "hidden" lesions of the rotator interval. *J Shoulder Elbow Surg* 1994;3:353-360
32. Bennett WF. Subscapularis, medial, and lateral head coracohumeral ligament insertion anatomy. Arthroscopic appearance and incidence of "hidden" rotator interval lesions. *Arthroscopy* 2001;17:173-180
33. Gerber C, Sebesta A. Impingement of the deep surface of the subscapularis tendon and the reflection pulley on the anterosuperior glenoid rim: a preliminary report. *J Shoulder Elbow Surg* 2000;9:483-490
34. Snyder SJ, Karzel RP, Del Pizzo W, Ferkel RD, Friedman MJ. SLAP lesions of the shoulder. *Arthroscopy* 1990;6:274-279
35. Hodler J. Technical errors in MR arthrography. *Skeletal Radiol* 2008;37:9-18
36. Gückel C, Nidecker A. The rope ladder: an uncommon artifact and potential pitfall in MR arthrography of the shoulder. *AJR Am J Roentgenol* 1997;168:947-950